

3D Gaze model during visual localization experiments using quaternions

Mathijs Prudon, s4486749

Under the supervision of Annemiek Barsingerhorn, Jesse Heckman and John van Opstal

Abstract

The biophysics department of the Radboud University of Nijmegen has decades of experience in research in the neuro-physics and mechanics of saccades, and other eye movements. Since a couple of years, a vestibular chair is being constructed to do research into the effects of vestibular stimulation on human subjects during localization of stimuli. To construct the gaze of a subject, head-in-world and eye-in-head data is measured using real-time camera tracking and modelling techniques. So far, the orientations of head and eye were simply added up to approximate the gaze, neglecting translational movements and torsional rotations of the head. This report attempts to find a method that does consider translations and 3D-rotations of the head, and calculate the gaze through matrix multiplication, to improve the gaze approximation. This is done by performing two experiments. One where the subject is asked to move their head in extreme orientations and positions while fixating their gaze at an LED, and one where the subject is tasked to locate stimuli while making radical and extreme movements with their head. By assuming that the subject's localization is accurate, which is a good approximation if the stimuli are displayed sufficiently long, the calculation method can be tested. Using Fick angles to construct rotation matrices, as done by Ronsse, et al. (2007), did not result in significant improvements. However, using quaternions to construct the rotation matrices, an improvement is realized for experiments where very extreme and radical head movements were made by the subject. But, if the subject moved their head orderly, these improvements were not visible as clearly. Further research must be conducted to prove the validity of the calculation of the gaze.

Introduction

Because humans are only able to perceive detail with a small area of the retina, called the fovea, we need to make frequent saccades to get a visual perception of the world. The response time, accuracy and speed of these saccades are undeniably remarkable, clocking in at over 500 degrees per second (Collewijn, Erkelens and Steinman, 1988). In the beginning of the twentieth century, the Dutchman Franciscus Donders and the German Johann Listing were the first to delve into the physiology of the human eye (Donders, 1864, Listing, 1845). In 1964, D. Robinson explored the mechanics behind human saccadic eye movements by building a model to describe the eye by its dynamical abilities and constraints, which formed the starting block for further research in the field (Robinson, 1964). Since then, research on the (human) eye has intensified. Nowadays, current technology gives us the opportunity to investigate the neurological and oculomotor

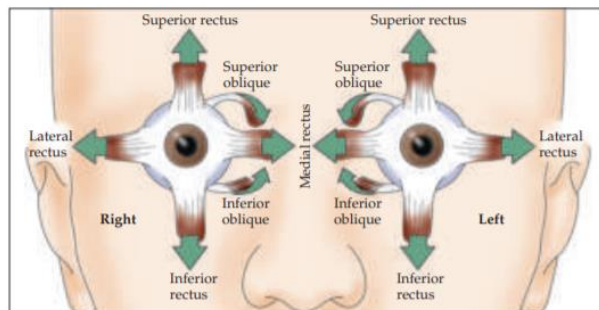


Figure 1 – This figure shows the anatomy of the muscles driving the movement of human eyes. For each eye the muscles can be placed in three sets of two, the lateral and medial rectus muscles, the superior and inferior rectus muscles and the superior and inferior oblique muscles. (adapted from Purves, 2008)

properties of the eye. This is of particular interest, because the eye is a sophisticated mechanical structure, directed by six distinct muscles per eye, able to rotate the eye in all three dimensions. This structure can be compared to other motor systems like the ones that control our limbs. The anatomy of the

muscles is shown in figure 1. The medial and lateral rectus muscles are solely responsible for horizontal eye movements, where the superior and inferior muscles, and the oblique muscles are responsible for both the vertical movements as rotations along the axis of gaze, known as cyclotorsion, or just torsion. The structure of the motor control of human eyes and the neurological structure responsible for this control has been mapped to great detail in past research (see e.g. overview by Spark, 2002). We now know that the saccade control in humans is directed from the superior colliculus (SC) in the brainstem and the frontal eye fields (FEF) in the frontal cortex (Brodmann-area 8) (Purves, 2008). In the SC, visual and auditory information gets translated into a code of electrical signals by information type specific cells (visual or auditory). Both types of stimuli are combined in the processing in the SC depending on timing and original location (Sparks, 1986). There is also some understanding on how the SC cells program the motor system. Past research found that the SC maps the motor controls in polar coordinates and that is anisotropic and nonlinear (van Opstal, van Gisbergen, 1989). Nearly 10 years later, Goossens and van Opstal (1997) visualized saccades to visual and auditory stimuli. With this data they proposed a 2D gaze control model on how saccades are produced. Axons of motor neurons in the SC reach to so-called gaze control centers, located lower in the brainstem; in the midbrain, caudal midbrain and pons. Horizontal and vertical saccade components are controlled through separate neuron control trains and are synchronized so that they are executed simultaneously. The paramedian pontine reticular formation (PPRF) is the gaze control center that is responsible for the horizontal component of saccades, directing the lateral and medial rectus muscles and the horizontal components of the superior and inferior oblique muscles. The control of vertical saccade components is conducted by the rostral interstitial nucleus of the medial longitudinal fasciculus (riNMLF). The information of direction and velocity of the

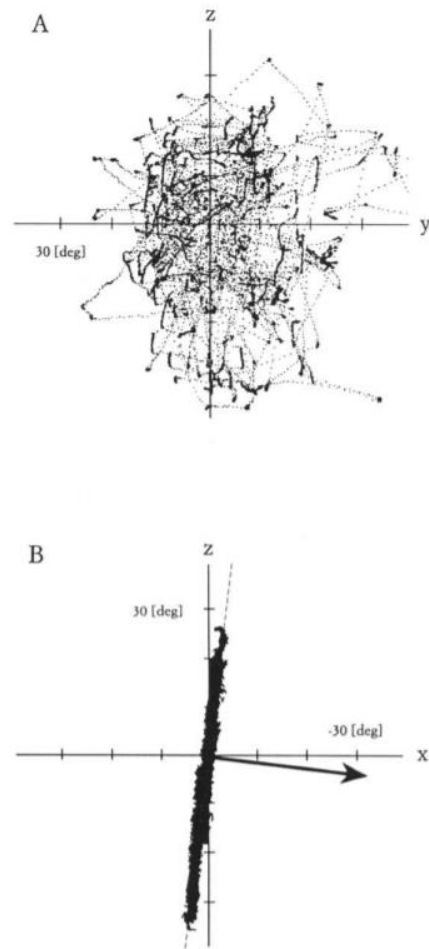


Figure 2 – This figure shows the endpoints of rotation vectors of arbitrary made saccades by a monkey for 90 seconds in the (A) horizontal (y) and vertical (z) component, and (B) vertical and torsional (x) component. Notice the clearly visible Listing's plane in graph B. (adapted from Haslwanter et al., 1991)

saccade that is to be made, is coded in the frequency, duration and number of spikes of the signals that the PPRF and riNMLF produce directed by the SC. Goossens and Van Opstal (2006) directly related the number of spikes by the SC to eye displacement in monkeys. The PPRF and riNMLF gaze centers connect to their own respective motor neurons that control the eye muscles. This entire discharge train is linked to the SC and not the FEF. The discharge train initiated by the FEF is to this day not well understood, but it is known that most control is done by the SC since a lesion in the FEF will be recovered over time while lesions in the SC are not recovered at all (Schiller, True, Conway, 1980). Sparks gives a detailed review about the

neurological structure of human eye movements in his 2002 paper (Spark, 2002; Purves, 2008).

Listing's and Donders law

The torsional rotation of the eye is just like the vertical rotation, controlled by the riNMLF, making the management of vertical and torsional rotation inseparable (Sparks, 2002). Moreover, as explained above, vertical and torsional rotations are conducted by the same set of eye muscles, which gives rise to a limitation to eye rotations during head-fixed saccades referred to as Listing's law. First derived by Johann Listing and later experimentally confirmed by Hermann von Helmholtz (Helmholtz, 1867) and directly measured in the 1980's (Ferman, Collewijn, Van den Berg, 1987), Listing's law states that the human eye cannot achieve all orientations and that all rotations initiated from a straight reference orientation are a result of a rotation around an axis laying in the plane orthogonal to the reference gaze orientation. This plane is called Listing's plane. This law only holds in the special case where the head is fixed and looking straight forward at a point infinitely far away. Under these unnatural conditions, all orientations that cannot be achieved with rotations about an axis within Listing's plane, the human eye is not able to make. Even then, the eye can still make small derivations from the Listing's plane, which are usually compensated in later saccades due to the eye position dependence of the neuron's activity in the SC (Van Opstal, Hepp, Suzuki and Henn, 1995). Listing's law is a special case of Donders law, which states that the 3D orientation is unique to the gaze direction. In other words, no matter how a certain gaze direction is obtained, the torsion will always be the same for a certain gaze. Under roll and pitch movements of the head and vergence of the eyes, Listing's law does not hold. This is comprehensible, because the torsion of the eye tends to counter the rotation of the head stabilizing the orientation of the eye in the world reference frame. Figure 2 shows a collection of rotation vectors

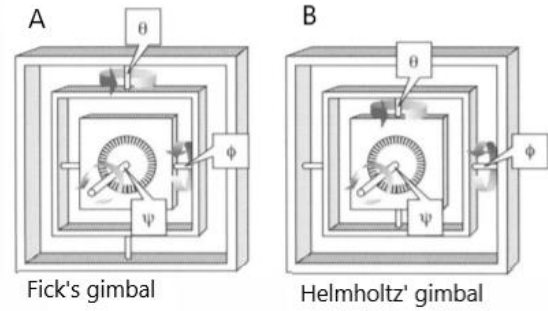


Figure 3 – This figure shows the clear difference between the gimbals made with (A) Fick angles and (B) Fick angles. The difference in order of rotations around the three axis will result in a different end orientation (adapted from Halswanger, 1995).

corresponding to 90 seconds of free saccades made by a monkey, while his head was fixated. In figure B, Listing's plane is clearly visible; all endpoints of the rotation vectors fall on or close to the dotted line (Haslwanter, Straumann, Hess, Henn, 1991).

Fick and Helmholtz angles

One way of modeling eye orientations is using rotation matrices. Euler's theorem, which states that every orbital orientation can be reached from any arbitrary initial orientation through a single rotation about a single fixed axis, is not the way a 3D eye orientation was described for a long time. The method used until the 70's of the previous century was the method of describing an orientation using a multiplication of a rotation matrix corresponding with every orthogonal dimension. By using the matrices

$$R_1(\theta) = \begin{bmatrix} \cos(\theta) & -\sin(\theta) & 0 \\ \sin(\theta) & \cos(\theta) & 0 \\ 0 & 0 & 1 \end{bmatrix} \quad (1)$$

for the horizontal rotation axis,

$$R_2(\varphi) = \begin{bmatrix} \cos(\varphi) & 0 & \sin(\varphi) \\ 0 & 1 & 0 \\ -\sin(\varphi) & 0 & \cos(\varphi) \end{bmatrix} \quad (2)$$

for the vertical rotation axis and

$$R_3(\psi) = \begin{bmatrix} 1 & 0 & 0 \\ 0 & \cos(\psi) & -\sin(\psi) \\ 0 & \sin(\psi) & \cos(\psi) \end{bmatrix} \quad (3)$$

for the torsional rotation axis, every orientation could be obtained by multiplying them in order, with their own respective angles. These angles are called Euler angles or Tait-Bryan angles and fully describe the orientation. Euler angles and Tait-Bryan angles differ in the fact that with using Euler angles, the first rotation axis is the same as the third, where for Tait-Bryan angles, all axes are used for the 3D rotation. A rotation of vector r_i around the horizontal axis with angle θ and vertical axis with angle φ to reach the new orientation r_f would then be written as

$$r_f = R_1(\theta) \cdot R_2(\varphi) \cdot r_i \quad (4)$$

To complete the information on the orientation of the eye, the torsional component must be added. Because of the non-commutative nature of 3D rotations, a problem arises with describing a rotation by the above described method. For 3D rotations the order of multiplication results in a unique orientation. Writing this out gives:

$$R_1(\theta) \cdot R_2(\varphi) \cdot R_3(\psi) \neq R_2(\varphi) \cdot R_1(\theta) \cdot R_3(\psi)$$

This specific order of multiplying the different coordinate and angle specific rotation matrices show the disagreement between Adolf Fick and Hermann Helmholtz, who, in the nineteenth century, disagreed which order was superior over the other. Later the scientific community started referring to the order of corresponding angles as Fick and Helmholtz angles respectively. Taking the order of rotation into account, the three Helmholtz or Fick angles fully describe the rotational orientation. Figure 3 visualizes the difference in order of rotation between Fick and Helmholtz with a so-called gimbal, a system where rotations about coordinate axis are carried out in sequence to reach a final position. (Haslwanter, 1995)

Quaternions

A way to overcome the problems that arise from defining rotation matrices by three angles

is to use a method that more closely resembles Euler's theorem. This can be done in the form of quaternions. The use of quaternions eliminates the importance of order when describing a single 3D orientation, but are still, just like rotation matrices, non-commutative. Mathematician William Hamilton discovered quaternions (Hamilton, 1844-1850), which are simply-said the extension to the imaginary number scheme that can unintendedly describe rotation in a very neat way. Quaternions extend the three-dimensional real world with not only one imaginary dimension i , but with three imaginary dimensions i, j and k . The rules that describes these dimensions are

$$i^2 = j^2 = k^2 = i \times j \times k = -1 \quad (5)$$

and

$$\begin{aligned} i \times j &= k & j \times k &= i & k \times i &= j \\ j \times i &= -k & k \times j &= -i & i \times k &= -j \end{aligned}$$

A quaternion is written similar to how imaginary numbers are written when only using one dimension, but then with the three imaginary dimensions:

$$q = q_0 + q_1 \cdot i + q_2 \cdot j + q_3 \cdot k \quad (6)$$

where q_0 is called the scalar component and $\{q_1, q_2, q_3\}$ is the vector part. For representing rotational orientations, unit quaternions are used (length 1 i.e. $\sqrt{q_0^2 \cdot q_1^2 \cdot q_2^2 \cdot q_3^2} = 1$). The relation between this type of quaternion and rotations that are described by a 3D rotation matrix is

$$q \circ (x \cdot I) \circ q^{-1} = (\mathbb{R} \cdot x) \cdot I \quad (7)$$

where q^{-1} is the inverse of the quaternion, x is an initial orientation vector, \mathbb{R} is the according rotation matrix and $I = \begin{pmatrix} i \\ j \\ k \end{pmatrix}$. For subsequent rotations described by quaternions, order once again uniquely describes the final orientation of the rotated body.

Rotation vectors

Rotations can also be described in a third way, called rotation vectors, which are tightly bound to quaternions. This method of describing rotations most closely resembles Euler's Theorem and is written as

$$r = \frac{q}{q_0} = \tan\left(\frac{\theta}{2}\right) * n. \quad (8)$$

In this formula the rotation vector is described as a vector r , rotated around the axis n with an angle θ , as Euler's Theorem describes. The rotation vector r can be turned into a rotation matrix by

$$r = \frac{1}{1+(R_{11}+R_{22}+R_{33})} \cdot \begin{pmatrix} R_{32} - R_{23} \\ R_{13} - R_{13} \\ R_{21} - R_{12} \end{pmatrix} \quad (9)$$

where the rotation matrix would then be

$$\mathbb{R} = \begin{pmatrix} R_{11} & R_{12} & R_{13} \\ R_{21} & R_{22} & R_{23} \\ R_{31} & R_{32} & R_{33} \end{pmatrix}.$$

(Haslwanter, 1995)

Modelling gaze

Many studies have been performed on gaze and eye saccades, testing multiple properties of the oculomotor systems of human subjects. Two main methods are used in past research to measure eye-head saccades. The first method consisted of two coils moving in large uniform magnetic fields, first proven useful by Robinson (1963) and later used by for instance Goossens and van Opstal (1997) and many others. One coil, attached to the head, was used to track the head position. The other one, embedded in a contact lens that was placed on the surface of the eye, tracked the position of the eye. Movement of the head and eyes would result in a change of measured magnetic flux, that could be translated to the actual movement of the head and eye thus measuring the eye in space and head in space. Finding the eye in head location, makes the analyzing of the accuracy and latency of gaze saccades possible. As technology evolved, optical tracking of gaze is now widely used in research and in commercial applications. In the past, before Robinson first

used the coil method in 1963, only optical methods were used to do research on eye movements, but without the use of computers (Wade and Tatler, 2005). In research, combining optical data with computer power to study eye movements was first used in 1987 (Vieville and Masse, 1987), and is now used widespread.

Eye tracking

Typically, there are three methods to track and compute eye orientations optically. One models either an elliptical shape or a complex shape to the eye or one of its features like the eyelids, iris or pupil, and can be categorized by the term shape-based approach. Orientations changes of the eye are then measured by the orientation changes of the model and a similarity measure, or confidence measure as used in this report, gives the reliability of the data. Another method is feature-based and measures orientation of the eye, based on certain distinct features of the eye, like the cornea reflections or the contrast differences in the image between the pupil or iris and the white of the eye. Another method that may be used is a template comparison, or appearance-based method. Here images get compared with templates to directly track the eye. This is subject to failure under rotations of the image or variance in scale. This method is based on statistics and needs a lot of training data. It is therefore not often used (overview paper by Hansen, 2010). Cesqui, et al., (2013) showed that using eye tracking technology can be more accurate than the electromagnetic one, considering that measures must be taken for slippage of the head gear during the experiment. Of course, the accuracies in his study are greatly dependent on precise calibration and settings of the parameters involved. A particular difficult part of obtaining 3D gaze is the torsion. Hatamian and Anderson (1983) where the first to show that cross-correlating images of the iris of a human is sufficient to find the torsion of the eye. At the time, the procedure of measuring was very time-consuming and error sensitive. The last decades numerous researches and

methods were proposed that improved these statistics. Currently, methods have been proposed that can measure torsion at 100 Hz, in real time, with an error of less than $0,1^\circ$ within a gaze of 20° up, left and right and 10° down (Otero-Millan et al., 2015).

Head tracking

For head tracking, two different methods can be used. The first is optical and uses optical light (usually infrared) to track either active LEDs or reflective dots. A ternary of points is enough to form a rigid body that could resemble the head, but more points may improve accuracy and therefore reduce the error margin. Head movement can also be measured by using an inertial movement unit or IMU, which measures movement relative to calibration parameters. This is however very sensitive to slippage that could render a measurement usage and thus must be calibrated frequently which could be impractical.

Gaze

A gaze can be constructed by combining head and eye data. This can be done in 2D and 3D. As described above, the human eye rotates in three dimensions but for some studies 2D gaze models are sufficient. 2D gaze models do not need sophisticated calibration and are easy to implement, but will fail under large head movements and do not give the complete picture of eye-head movements. 3D gaze is defined by horizontal rotations, vertical rotations and torsional rotations of both the head and eye. 3D gaze models do give the full picture but are geometrically much more difficult to implement due to the non-commutative nature of 3D rotations. Also, since the head movements displace the position of the eyes and the head rotates around different axes as the eyes, the analysis of the gaze direction of the subject and the 3D orientation of the eye from the data, turns into a complex geometric problem. In the previous section three methods of defining rotations are described. Cesqui et al. (2013) solved the

geometric problem in his paper by introducing five reference frames, one for the data of the eye tracking camera and one for the data of the head tracker, one for the eye and one for the skull and one for world frame. By constructing angles and associated rotation matrices from the coordinates obtained from the trackers, and translating them to the right reference frame, Cesqui et al. could obtain an accurate unrestricted gaze of the subject in the world frame. Using Fick angles to construct rotation matrices for head and eye has also been proven a viable method of determining gaze (Ronsse, Oliver, Lefèvre, 2007). With such a method it is important to take the order of angles into account to prevent problems described in the above section on Fick angles. The usage of quaternions to describe gaze orientation has also already been proven (Tweed, Cadera and Vilis, 1990) with its above described advantages over using Fick angles. Because of the smaller size of quaternions, only four numbers define a quaternion while a rotation matrix needs nine, another big advantage of using quaternions is computing speed. The use of quaternions becomes even more advantages when performing operation like multiplication (Huynh, 2009).

The goal of this study is to find a robust calculation method for determining gaze in the reference frame of a movable chair for unrestricted head and eye movements using a head-tracker and pupil detection hardware and software. The goal is, that this method can then be used for later research in localization experiments under vestibular stimulation.

Methods

To check the accuracy of our analyses, a variety of experiments were conducted. All experiments were conducted in a movable spherical mainframe structure with a chair located in the middle, from now referred to as the vestibular chair (see figure 4). With this chair, localization experiments can be conducted under vestibular stimulation. In our

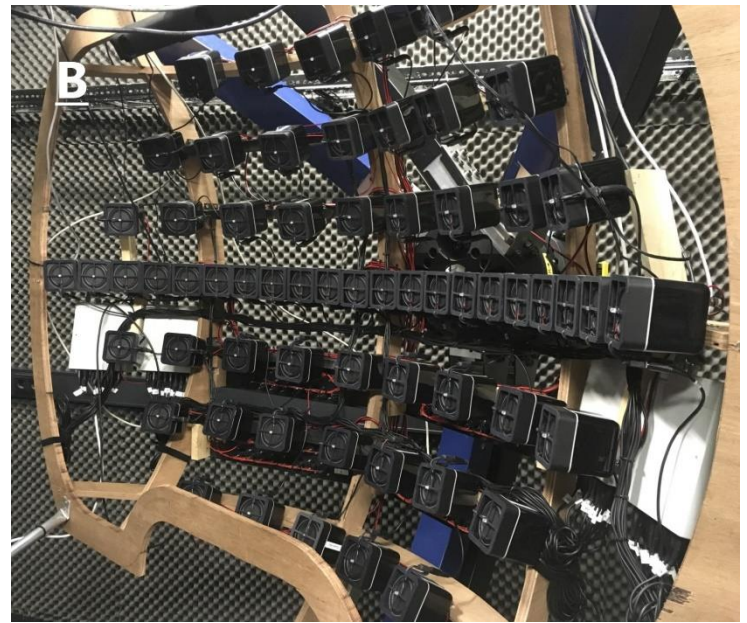


Figure 4 – A: This image shows the structure of vestibular chair. The black beam structure can be rotated about the vertical axis and the blue beams can be rotated about the horizontal axis. (www.ru.nl) B: This image shows the hemisphere of the 63 speakers and LED's with the middle one being the fixation LED. (www.mbfys.ru.nl)

experiments the chair was kept stationary. The vestibular chair was situated at the biophysics labs of the Donders Institute for Brain, Cognition and Behavior at the Radboud University Nijmegen. In front of the chair, 63 speakers with built in LEDs were attached to a wooden hemisphere in a range of -50 to 50 degrees in azimuth and elevation relative to the middle speaker. This middle speaker is referred to as the central fixation LED and is situated at coordinates (0,0) in azimuth and elevation. Above this hemisphere Optitrack's hardware is hung up, made up from three infrared cameras (OptiTrack V120 trio System, www.optitrack.com). A collection of computers is hung behind the backrest of the seat that collected the data during experiments. Figure 4 shows the setup. All experiments were conducted on two subjects; KW and MP. Both subjects have normal vision and no refractive error in their eyes. More hardware from OptiTrack was used: Five active infrared LEDs were mounted on a headband and were defined as a rigid body and tracked by Motive, OptiTrack's software. Via trigonometry the

orientation and location of the rigid body were determined and saved on one of the computers on the backrest of the seat. A relatively arbitrary ground plane was defined just below the straight line of sight, with the y-axis oriented upwards, the x-axis oriented to the right and the z-axis oriented to the rear, relative to the straight line of sight (see figure 5A). The eye orientation was measured with PupilLabs software and hardware (Core glasses, Pupil Labs GmbH, www.pupil-labs.com). The hardware was made up of a frame that most closely resembles the frame of a pair of glasses and was worn by the subject. It was equipped with a world-camera mounted on the frame, above the right eye, and an eye-camera mounted on an adjustable beam in front of and below the right eye. The software used the shape-based method to track the pupil, as described in the introduction. It fits an ellipse to the pupil contour and uses a 3D model to determine a normalized orientation vector. Before every measurement with the PupilLabs eye tracker, a calibration procedure must be performed. A unique high contrast marker was held at

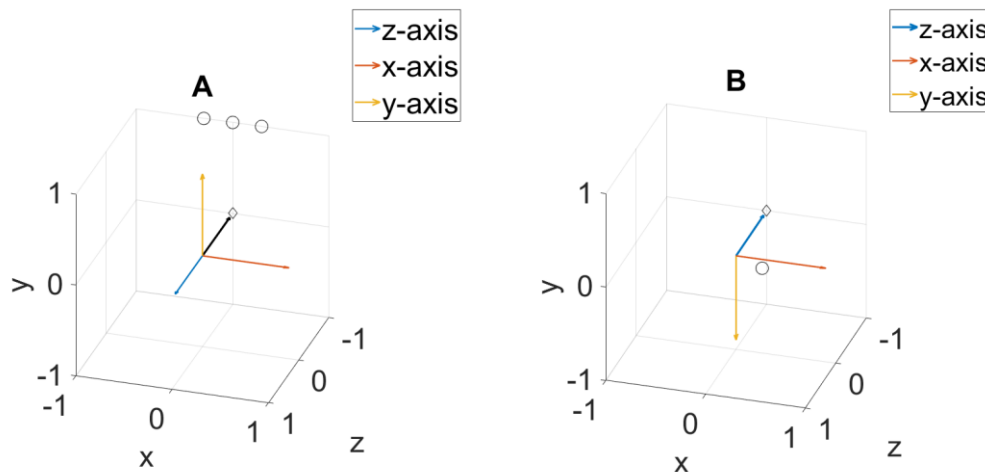


Figure 5 – (A) This figure shows the axis of Optitrack’s coordinate system in its own reference frame. The blue arrow denotes the z-axis, the red arrow the x-axis and the yellow arrow the y axis. The black arrow denotes a straight gaze toward the fixation LED (black diamond). The three black circles show the location of the cameras in front and above of the subject. The origin is the location of the eye. **(B)** This figure shows the coordinate system of PupilLabs’ data within the reference frame of Optitrack’s data. The colored arrows denote the same coordinate axes as in A. In this coordinate system the z-axis points towards a straight gaze toward the fixation LED (black diamond). The black circle is the camera that films the eye suspended to the right and just below the eye. The eye is **ones** again located at the origin.

armlength in front of the subject to look towards while moving their head in different orientations. The calibration could be checked by viewing the live image of the world camera where a point should be displayed where the subject looks at. If this was correct, the calibration was successful. The software also gave an accuracy and precision parameter that could be used to check the calibration. A value for the accuracy parameter of two degrees or less was interpreted as accurate. The reference frame of the eye tracking was oriented as follows; the x-axis oriented to the left, the y-axis oriented upwards and the z-axis oriented straight ahead, relative to the line of sight for a straight gaze. See figure 5B for a visualization of this coordinate system in the reference frame of Optitrack’s data.

Central fixation experiment

To test whether the analyzing script modulates the gaze correctly, two experiments were conducted. One of these was a central fixation experiment. During this experiment the subject

was tasked to keep their gaze on the fixation LED for a predetermined amount of time (three blocks of 1 minute). During this time the subject made arbitrary translational, rotational and torsional movements with their head, while keeping their gaze at the fixation LED. The goal of this experiment was to test the script for correctness in calculating the total gaze for a variety of extreme head movement. The subject was free to move their head; no instructions were given besides that every orientation was allowed. The resulting gaze calculation should be approaching a constant gaze over time at the fixation LED, thus nearing 0 degrees for both coordinates azimuth and elevation. The PupilLabs hardware is a lot more sensitive than the Optitrack hardware. Because of sporadic low confidence values for the pupil tracking and because of vergence of the eyes, we assume that an error of 3 degrees could be a result of an error in the measurements.

Localization experiments

The second experiment was a collection of localization experiments, with one under extreme orientations and translations of the head. During normal localization experiments, when testing the capability and limits of humans during stimulus localization under different light conditions or during vestibular stimulation a LED only must be lit up for a few milliseconds. To test our script these human limits were not of our interest, only the validity of the analyzing script was. The LED stimuli were therefore shown for long enough to make sure the subject could locate the target (i.e. a second or more). For all localization experiments, first the fixation LED was lit up, so the subject made saccades initiated from the same orientation for every saccade. After this, the stimulus LED was lit up. We started by conducting a localization experiment where the subject was tasked to only move his eyes and keep the orientation of their head fixated towards the fixation LED. After this the same experiment was conducted where the subject was instructed to move both their eyes and head, performing saccades in a natural way. The final localization experiment was conducted under extreme head movements and orientations. The subject was, similar as during the fixation experiment, instructed to make extreme translational and torsional movements with their head during the localization of the stimuli. Because of the length of time the stimuli were shown the experiment, this should still result in an accurate localization by the subject and therefore tests the script for correct computation of the gaze of the subject.

Analyzing

The analyzing scripts were written in Matlab, version R2018b. Firstly, Ronsse's method was used (Ronsse et al., 2007). This method used defined Fick angles determined by the orientation of the rigid body that resembled the head to construct rotation matrices, which in their turn were computed into a final gaze vector (see introduction). The script was first

written for the manual input of values for head orientation, eye orientation and eye location relative to the initial position. This data was used to compute a gaze vector using the rotation matrix used in Ronsse's paper (Ronsse, et al., 2007). After constructing of the gaze vector, the vector was intersected with a hemisphere defined by the location of the central LED, which was located at the coordinates (0.1257; 0.0195; -0.8426) in the Optitrack reference frame (see figure 5 for indication of this setup). This location was determined by attaching trackable points to a laser pointer that measured the distance between itself and the fixation LED. The location of the laser pointer was determined by Motive, and with the distance read out on the laser pointer, the location of the fixation LED in the Optitrack reference frame could be found. The intersection coordinates were then used to compute the azimuth and elevation via the geometric properties of the hemisphere. The script is given in the appendix.

After simulations to check that filling in different values for location for the eye and orientation of eye and head gave the correct results, the script was applied to real data. Motive tracks the head orientation and exports the data in quaternions and location data in cartesian coordinates in OptiTrack's reference frame. This location data could be used since the hemisphere is also defined in OptiTrack's reference frame. The quaternions must be converted into Fick angles which can be done by defining an order of rotation over the three coordination axes, which in the case of our Fick angles and the reference frame of Optitrack, was 'zyx' or '321'. If this order was altered, the final values for azimuth and elevation were different and therefore incorrect (see introduction).

After intensive testing, the script was adjusted to not construct the rotation matrices with Fick angles, but with quaternions (equation 7). This had the convenient advantage of eliminating the problems that arose from the conflicting reference frames which made the construction

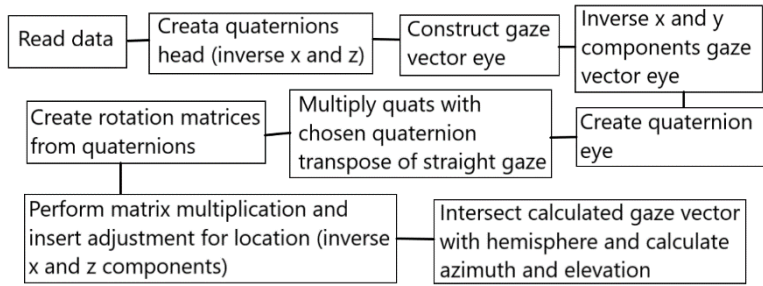


Figure 6 – This scheme shows the different steps taken in the script, using quaternions to create rotation matrices. For the full script, see the appendix.

of rotation matrices with Fick angles tricky. Also, the problem of order in constructing the Fick angles out of the quaternions was eliminated. Now only the x-axis and the z-axis must be inverted due to the difference in reference frames between Optitrack’s and PupilLabs’ data. The output data PupilLabs’ software produces, was a normalized gaze vector. By defining the straight gaze as a vector $(0,0,1)$, a rotation matrix could be estimated. Then a normal vector could be calculated about which the rotation takes place by

$$\mathbf{n} = \mathbf{r} \cdot \mathbb{R} \quad (10)$$

where \mathbf{r} is the normalized gaze vector and \mathbb{R} is the estimated rotation matrix. Then the quaternion resembling the rotation could be determined using equation 8. To calibrate a straight gaze the quaternion data must be multiplied by the inverse of the quaternion that was known to resemble the straight orientation. This was done by looking at the raw orientation data of the eye and head and manually choosing a moment in time where this was the case. By asking the subject to look straight when initiating the experiments and building in a pause between starting the measurements and showing the first LED stimulus, these moments of straight gaze could always be found. Figure 6 gives a scheme of all the steps done to get to the results.

Reference frames

Looking to figure 5, it is obvious that the different reference frames involved must be aligned. To align them, for the head data

(Optitrack), the x and z data can be inverted to rotate the frame 180 degrees about the y-axis and create a logical reference frame seen from the subject. To align both reference frames, for the PupilLabs data the y and x data needed to be inverted as well. Then what remained, was that for the location data to be correct as well, the x and z data needed to be inverted too. For

the quaternion calculation, this is easy to implement (see script), but for the Fick angles method this is not. For the Fick angles method, all cartesian location data was inverted to obtain the results. This is further discussed in the discussion section.

Results

Fick angles

To check our method, we first performed simulations to visualize the experimental setup for a single moment in time. By filling in the orientation of the head in 3D (azimuth, of the elevation and torsion), the orientation of the eye in two angles, azimuth and elevation, and the location of the eye in cartesian coordinates relative to the middle of the hemisphere formed by the speakers and LED’s, a gaze vector was calculated and displayed which intersects the hemisphere at the red cross (see figure 14 in the appendix). From the intersection coordinates a gaze was computed in polar coordinates, using geometrics of the hemisphere, so they could be compared to the stimuli’s polar coordinates during the fixation experiment. The results of implementing this visualization method is shown in figure 7 for both subjects MP and KW. The plotting of the visualization for all data points was computationally very intensive and therefore omitted for the calculation of gaze for the data of the experiments. The location data is relative to a straight gaze. The figure shows the gaze as a function of time for both the azimuth and elevation. Both the calculation method as

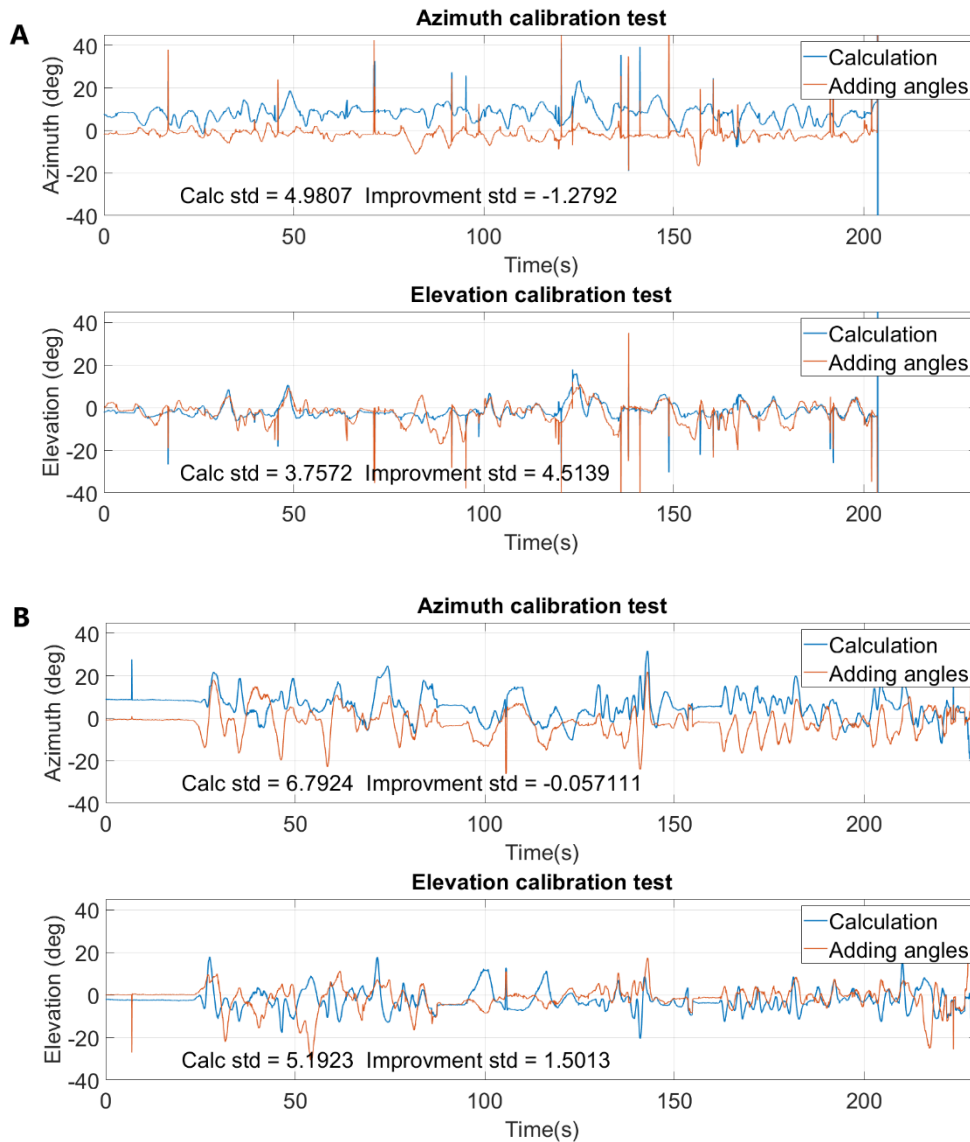


Figure 7 – This figure shows the gaze over time during the fixation experiment, where the gaze is calculated using Ronsse's method with Fick angles (blue line) compared to the gaze constructed from adding the angles of orientation of head and eye. **A** shows the experiment conducted on subject KW. **B** shows the experiment conducted on subject MP. The standard deviation of the gaze calculated with Fick angles is shown in the figure as "Calc std". The improvement of this standard deviation over the one calculated by adding angles is shown as "improvement std".

explained by Ronsse, et al. using Fick angles (blue line) and simply adding the angles of orientation of the head and eye (orange line) are plotted. The adding angle method does not take translational and torsional movements of the head into account. As visible in the figure, for elevation our approach resulted in an improvement of the standard deviation of about 4.51 degrees for subject KW and about 1.50 degrees for MP compared to simply adding the angles of head and eye. For the azimuth

direction the standard deviation gets worse for both subjects by about 1.28 degrees for KW and about 0.06 degrees for MP. Also, the absolute standard deviations are not within the desired limits of 3 degrees for both subjects, that could be explained by measurement errors. For KW the standard deviation for azimuth is about 4.98 degrees and for elevation is about 3.75 degrees. For MP the standard deviation is about 6.79 degrees for azimuth and about 5.19 degrees for elevation. For elevation the method seems to

be a step in the right direction, but for azimuth, just adding the angles of orientation is a better approximation which should not be the case. This problem, together with the increased speed of computing, leads us to use quaternions to try and improve the results.

Quaternions

Where with the use of Fick angles the script would run for nearly 90 seconds to complete the calculation of polar gaze for about 30000 datapoints, the use of quaternions to create rotation matrices would only take about 2 seconds to do the same. Further analysis will therefore be done using this method. The same data of the fixation experiment was analyzed

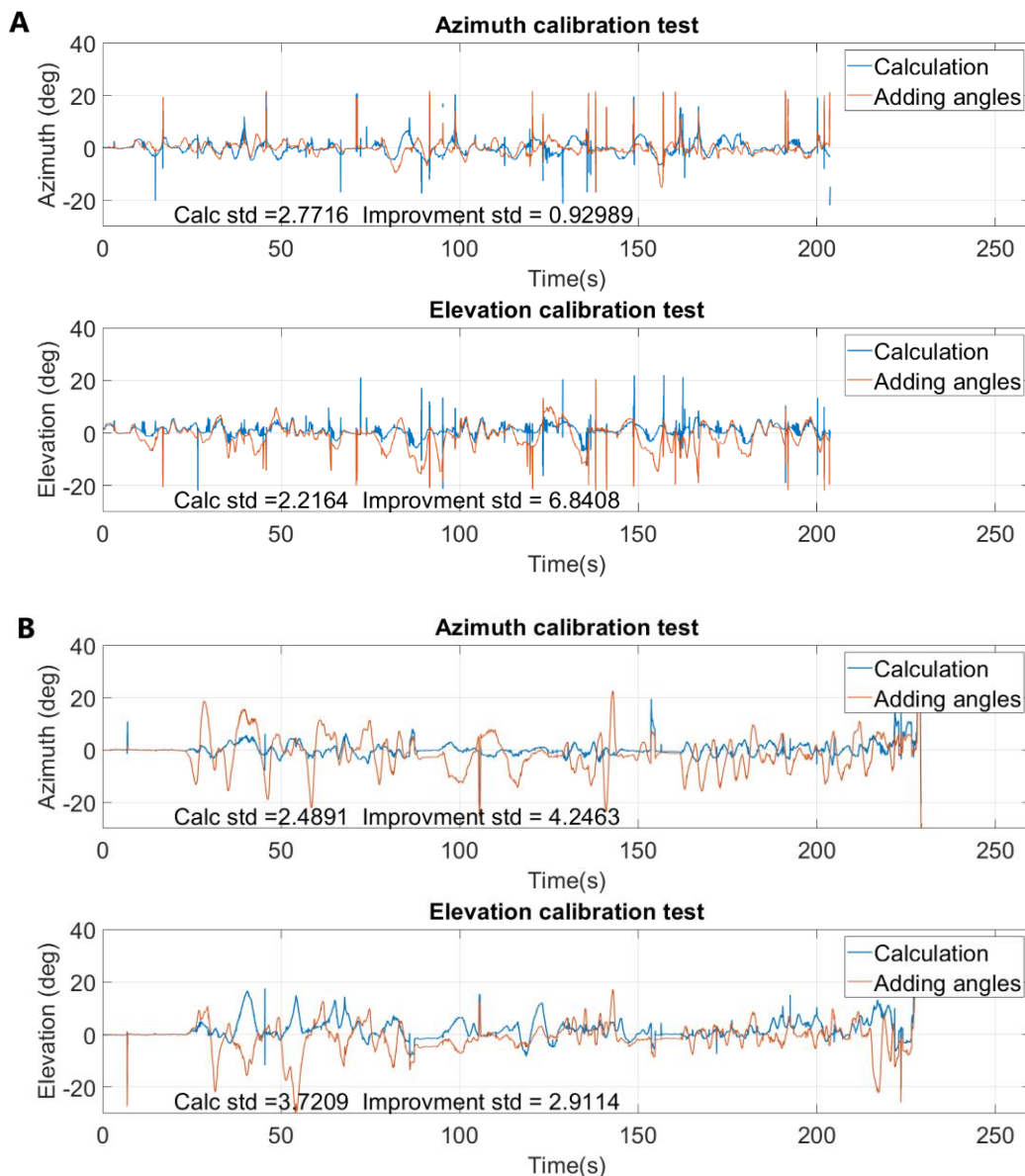


Figure 8 – This figure shows the gaze over time in azimuth (top) and elevation (bottom) of subject KW. Here the subject was tasked to keep fixation on the central LED (azimuth and elevation at 0 degrees). The red line gives the gaze given by adding the orientation of head and eye. The blue line gives the gaze by multiplying rotation matrices constructed with quaternions. It is expected that the gaze would remain at 0 degrees for both polar coordinates during the entire duration of the experiment. The standard deviation of the calculation line (blue) and the improvement of this standard deviation over the adding angles line (red) are displayed within the graph. **A** shows the data from subject KW, **B** shows the data from subject MP.

using this method. The results of this method are shown in figure 8. As shown for subject KW, there is a significant improvement visible for the standard deviation of the gaze for this experiment, with an improvement of about 0.93 degrees to a standard deviation of about 2.77 degrees for the azimuth, and an improvement of about 6.84 degrees to a standard deviation of about 2.22 degrees for the elevation. These values lie within the desired standard deviation of about 3 degrees. Still, there are peaks and dips that are larger than 3 degrees. For subject MP the improvements are similar for azimuth. For elevation the improvement seemingly is a lot smaller. The standard deviation of the gaze calculated with matrix multiplication is here about 3.72 degrees. Also visible, are some maxima that near 20 degrees, especially in during the first 80 seconds of the experiment. The thin peaks that are visible are due to blinks or faults in the pupil tracking.

Localization experiments

Three different types of localization experiments were conducted (see methods). The last experiment performed, where the subject was tasked to make arbitrary and extreme head movements during the localization, is the one where the difference between the original method of defining gaze of just adding the angles of head and eye orientation and the new calculation method using quaternions should be greatest and

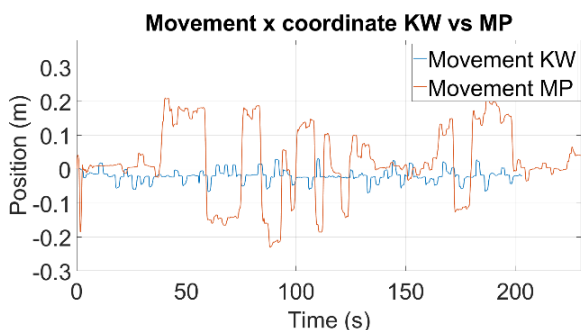


Figure 9 – This figure shows the movement of the subject's head in the x (horizontal) coordinate plotted against the time. The movement is shown over the whole experiment. The orange line represents subject MP and the blue line subject KW.

therefore the one that will be discussed here. For the first two experiments, no significant difference was found. Figure 9 gives an indication of the movements subjects KW and MP made with their heads in the last experiment. As seen in the figure, for the x coordinate, MP made far more extreme movements compared to KW. This is similar for the y and z coordinates. One can plot the gaze as a function of time for the adding angles method and the new calculation method for both azimuth and elevation where the stimuli are indicated in the graph by black horizontal lines (see figure 12 in the appendix). This figure may be difficult to read quantitatively. For some saccades the calculated gaze seems to be a better approximation than the gaze constructed by adding the angles, but for others it seems to be worse. This can only be concluded assuming that the subject's ability to accurately localize stimuli is perfect due to the length of time the stimuli are shown. To further evaluate the newly introduced script, let us look closer at single saccades, that either improve the gaze approximation or worsen it. Firstly, let us look at examples of improvement. Figure 10 shows three examples where the calculated gaze using matrix multiplication is a better approximation than the adding angles gaze. Figure 10A is the saccade made by subject KW at a stimulus of about 21,5 degrees to the left. Only the azimuth is shown here. By only adding the angles the gaze appears to be underestimated. While locating the stimuli, the subject simultaneously moved their head closer to the stimuli (shown in the lower graph of figure 10A) which means that she must adjust her head and eye orientation to locate the stimuli and make a smaller saccade. The new calculation takes this translation of the head into account and therefore approximates the gaze more accurately. This phenomenon is even better visible in figure 10B and C, which are saccades made by MP. In figure 11B, the subject's head position is moved to the left (the same direction as the stimuli) by nearly 20 centimeters, resulting that adding the orientation of head and eye would result in a

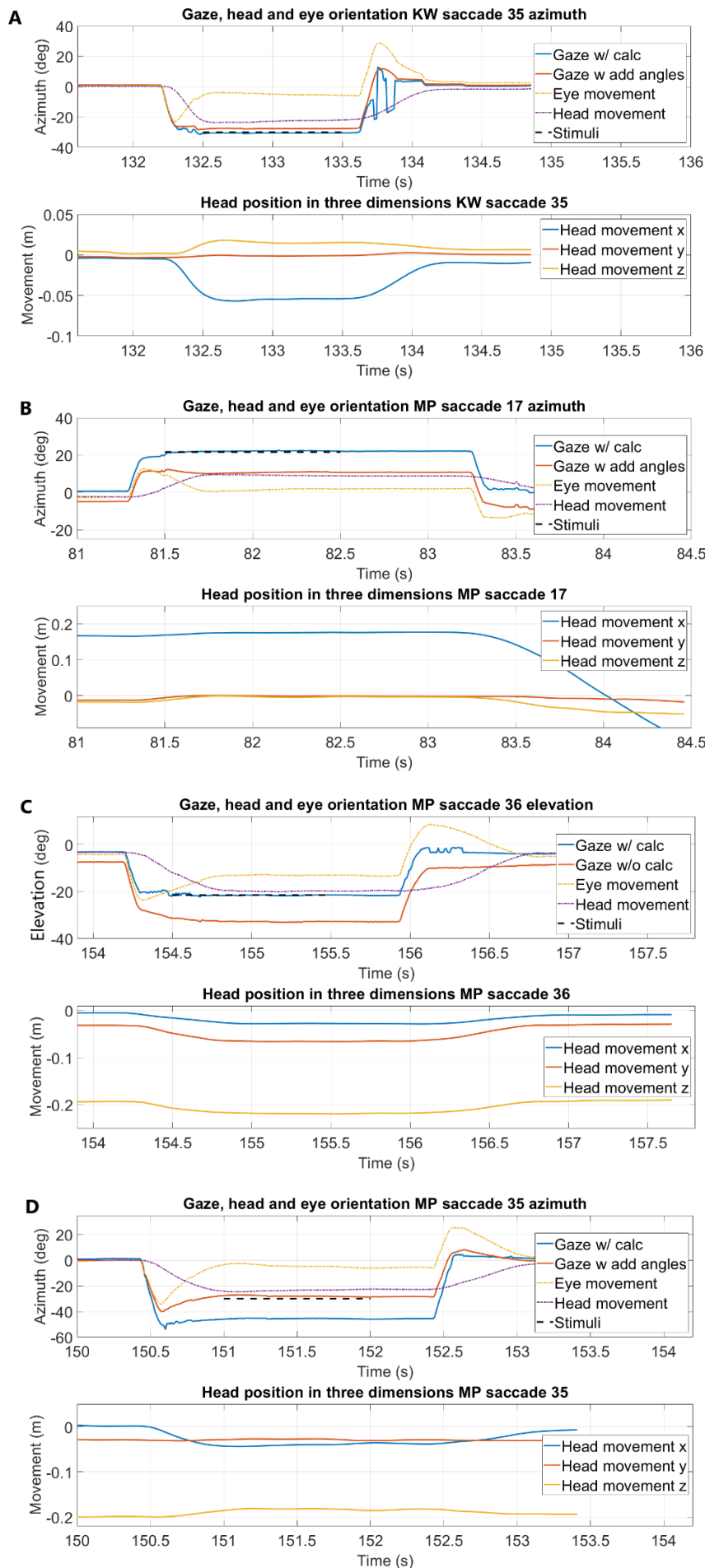


Figure 10– This figure shows a multitude of individual saccades. In every figure (A-D) the top graph shows the orientation of head, eye and gaze for a single saccade. All saccades are taken from the experiment where the subjects were tasked to make extreme head movements during the localization of the stimuli. The blue line is the gaze calculated with multiplying rotation matrices versus the red line which resembles the gaze constructed by simply adding orientational angles. In the top figure the orientation of the eye and head are also displayed in respectively a yellow and purple dotted line. The stimuli location is shown in a thick black dotted line. Note that the location of the stimuli is exact, but the timing is not resembled by the dotted line. It is only plotted for reference of accuracy of localization. For all lines the orientation in azimuth or elevation (depending on the saccade in question) is plotted against the time of the experiment. The lower of the two graphs displays the position of the head in three dimensions relative to an initial straight gaze position. Here the blue line is the x coordinate, the red line the y coordinate and the yellow line the z coordinate. **A** shows the azimuth part of saccade 35 made by subject KW. **B** shows the azimuth part of saccade 17 made by subject MP. **C** shows the elevation part of saccade 36 made by subject MP. **D** shows the azimuth part of saccade 35 made by subject KW. This is the only saccade of the four, that is an example where the quaternion calculation is worse than the adding angles calculation. All saccades shown are indicated in figure 11 which gives an overview of the experiment.

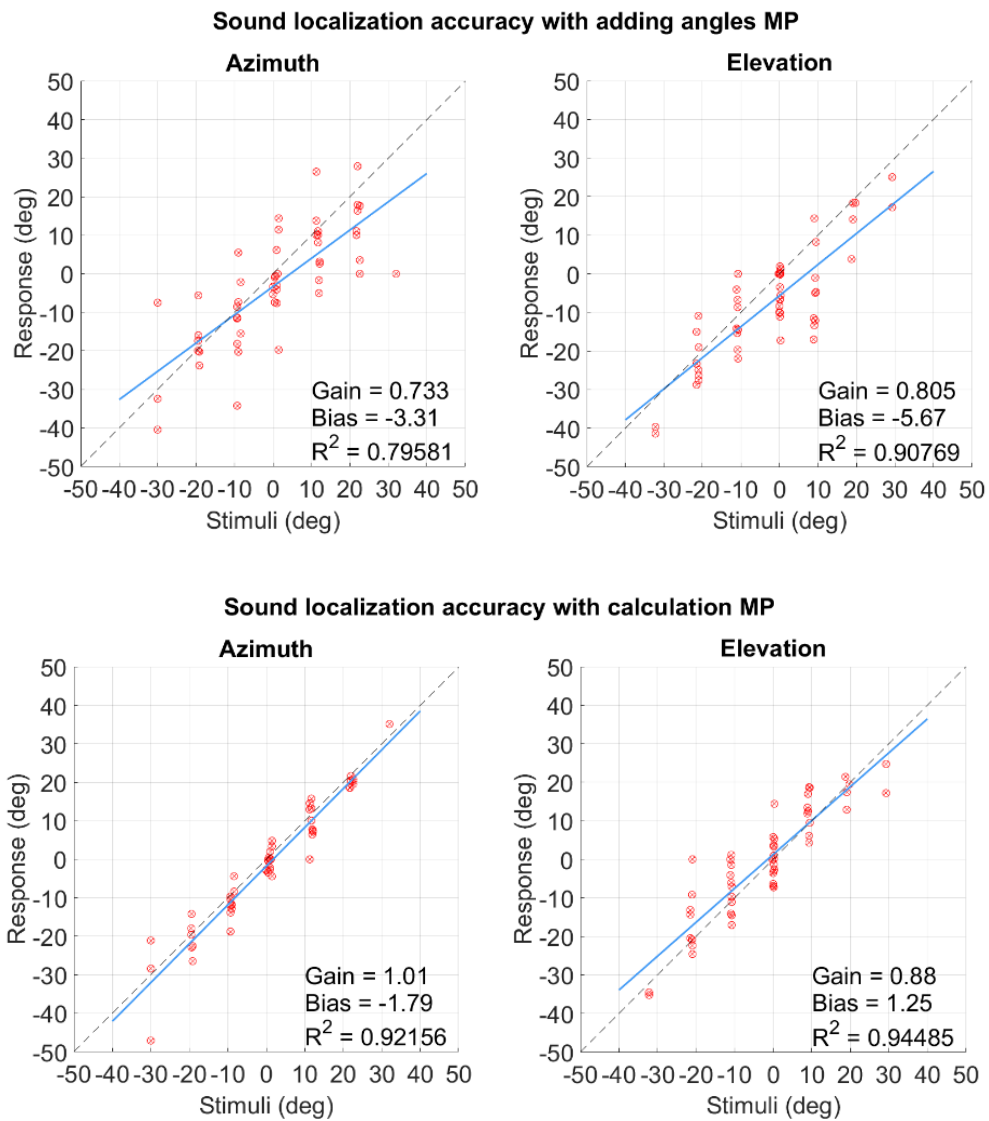


Figure 11 – This figure shows the accuracy of localization of subject MP during the localization experiment where the subject made extreme translational and torsional movements with their head. The response location is plotted against the stimuli location in degrees, both for azimuth (top) and elevation (bottom). The regression line is visible in blue with a dotted black line as the expected regression line. Values for gain, bias and R-squared are added to compare the figures quantitatively.

smaller deviation for the gaze in the reference frame of the hemisphere of speakers and LEDs. Where the calculation method takes this into account, the adding angles method does not, thus underestimating the stimulus. For C the opposite happens. Here the gaze in the hemisphere reference frame is much smaller than the orientation of the head and eye combined, since the subject has moved his head towards the negative z-direction, causing the adding angle method to overestimate the stimulus. These examples show that, under extreme head movements, different gaze angles are necessary to find the stimuli. Figure 10D shows an example where the adding angles

method is a better approximation than the new calculation method, again assuming that the subject's accuracy in locating the stimulus was perfect. The calculated gaze, using rotation matrices, underestimates the location of the stimuli. Here the subject (KW) moved her head about 4 centimeters frontwards and downwards, simultaneously with the saccade. The explanation for this error, and the ones in other saccades are discussed in the discussion. The saccades plotted in figure 11 are indicated by circles in figure 12. The location data in the lower graphs of figure 11 are in the Optitrack reference frame (see figure 5A). To give an overview of whether this new calculation

method in its current state, is better or worse than the approximation made by just adding the orientational angles of head and eye, one can use the assumption that the localization accuracy of the subject is perfect. With this knowledge, an accuracy plot would give insight in whether the new calculation method is an overall improvement. These accuracy plots are shown in figure 11 for MP and figure 13 (see appendix) for subject KW. A linear regression line is plotted and the gain, bias and R-squared are shown for the different methods. As shown, all parameters show an improvement for the calculated method relative to the adding angles one for MP. Especially for the azimuth the improvement is spectacular, showing a gain of 1.01 for the matrix multiplication method compared to 0.733 for the adding angles method. Also, the R-squared shows an improvement from 0.796 to 0.922. For the elevation the improvement is smaller; for the gain from 0.805 for adding angles method to 0.88 for the matrix calculated method, and for the R-squared 0.908 for adding angles to 0.945 for the matrix calculation method. For subject KW (see figure 13 in the appendix), the improvements are much smaller. The gain for azimuth shows an improvement of 0.061 and the R-squared value an improvement of about 0.02. For the elevation the gain actually decreases for the matrix calculation method relative to the adding angles method. The R-squared does show a small improvement.

Discussion

The method previously used, where orientation angles were added, is **physically** not correct. Matrix multiplication, however, is **physically** correct and should therefore show better results when calculating and plotting the gaze. Besides this, the old method does not include translational movements of the head and is only valid to this aspect if the eye remains at the exact same position during all saccades. This is not realistic, since the eye moves through space as the head rotates. Also, torsional rotations of the head are not accounted for in the old method but are in the new matrix multiplication

method. In this report, it was not researched which of these differences cause the improvements that are shown. Since the improvements in the accuracy plot are much greater for subject MP than for subject KW, and it is shown that subject MP made much more extreme translational movements with **their** head, it is no unfounded assumption that the improvements are mostly due to the inclusion of location data of the head. Below, both experiments and analyzing methods are discussed.

Fick angles

For the fixation LED experiment, the Fick angles method does not show the expected improvement (figure 7). It has been previously proven that this method is a valuable way to calculate a gaze vector for unrestricted head and eye movements, as Ronsse, et al. showed (2007). We did not manage to reproduce the same results in our setup. The standard deviation does seem to improve for the elevation coordinate of the gaze, but for the azimuth an improvement is not realized. Also, the absolute standard deviations for both the elevation and azimuth for both subjects MP and KW are greater than expected. These issues imply that the reference frames of Optitrack's and PupilLabs' data do not line up. For construction of the rotation matrix with the Fick angles, lining up the reference frames is not trivial. It is very easy to intermix reference frames and lose track of coordination systems while constructing rotation matrices this way and is therefore very error sensitive. This is further confirmed by the fact that the results were best, if all location data is inversed. As described in the methods, this is not expected. This makes for a far from robust, and maybe even fragile, script. It is more argumentative that the z and x-data need to be inversed since that would be the correct conversion to align the reference frames, as described in the methods section. This, in combination with the fact that the results are not as good as expected and the advantageous speed of computation with quaternions, caused us to divert to the use

of quaternions to create rotation matrices, instead of Fick angles, to do further analysis.

Quaternion calculation

Let us first discuss the fixation experiment. Here the standard deviation is smaller in all cases for the calculated gaze compared to the adding angles method (figure 8). It is interesting to note that the improvement for elevation is much greater than the one for azimuth. One may think that this is because for all experiments, the location of the eye is approximated at a central point in the middle of the active LEDs attached on the head band. However, because a straight gaze is also determined relative to this point, this explanation can be excluded. It is more likely that this difference arises from the fact that for elevational rotations (about the x axis in Optitrack's reference frame) of the head, the eye lies further away from rotation axis than for azimuthal rotations (about the y axis in Optitrack's reference frame) of the head. For the calculation with quaternions, the expected inversions need to be performed to obtain the best results. The triviality of inverting axes is a big advantage of this method, compared to using Fick angles. The resulted absolute standard deviations are within the expected value for a standard deviation of 3 degrees, but as can be seen in figure 8, has still some big peaks and dips that exceed this value. As will be discussed further in this chapter, the script is probably not perfect. Improvements can and must be made to deliver a robust gaze calculation. By looking at the movements, the subject makes at the times where the gaze deviates from 0 degrees, particular the location and orientation data of head and eye separately, one may be able to investigate what movements and orientations causes the gaze to deviate, and debug the script further to improve the end result.

Localization experiments

Three types of localization experiments were conducted. The first two, the one where the

subject was instructed to only use their eyes to locate the stimulus, and one where the subject was instructed to make only necessary movements with head and eye to complete the saccade towards the stimulus, do not result in differences between the adding angle method and quaternion calculation method. The interesting experiment to discuss is the final one, where the subjects made extreme translational and orientational movements with their heads while locating the stimuli. As showed in the results, we took a closer look into single saccades and compared the old adding up and new multiplication method. As described in the result there are a multitude of examples of single saccades where the quaternion calculation is a big improvement. Here the script seems to make the right corrections. But there are some stimuli where the script does not make the right corrections as seen in figure 10. For subject KW, in the elevation graph (bottom), the calculation method seems to undershoot the lower stimuli (Figure 12A). This is not the case for MP. Also, visible in the range between about 50 and 80 seconds in the azimuth graph for MP, where the movements made by MP are very extreme (evidenced by the fact that the adding angles method fails completely for this range), the calculation method is, although an improvement over the adding angles method, not accurate enough. Also, the fixation between stimuli, which should be at 0 degrees for both azimuth and elevation, is not at 0 degrees for this range. This is also the case for MP in the elevation graph between about 140 and 170 seconds. In this last case, looking back at the world camera video, it was found that between 140 seconds and 170 seconds subject MP moved his head forwards. Further investigation, for instance by doing an experiment where the same localizations are conducted for different head position, could determine whether this is a constructive error or a one-off error. The final result shown, the localization accuracy figure for subject MP (figure 11), shows a clear improvement in the regression parameters. For KW the improvement is not that clear (Figure 13

in the appendix). A reason why the improvement is clearer for MP in this plot, is probably because MP made more extreme head movements compared to KW (see figure 9), implying that the matrix multiplication method to construct the gaze as it stands now, is a better method to calculate gaze, but only for very extreme head movements during the experiment. If head movements are more orderly, an improvement could not be realized with the current calculation method.

Conclusion

Overall it can be concluded that we did not manage to implement matrix multiplication with rotation matrices constructed with Fick angles correctly. There is no clear improvement over just adding angles of orientation, even though it has proven before that it can work (Ronsse et al., 2007). Due to the non-commutative nature of 3D rotations, conflicting reference frames, data formats outputted by the measurement software and increased computation speed (Huynh, 2009), we shifted to a new method using quaternions to create the rotation matrices to do the multiplication with. With this method, improvements over the old adding method were realized for localization experiments where the subject performed very extreme and radical head movements and (torsional) rotations. For more orderly head movements during stimuli localization experiments, improvements were not clearly visible. Faults in the script and calculation method cannot be excluded at this time, so further research with more subjects need to be carried out to make the script robust and useful. Also, to construct the full 3D gaze, ocular torsion must be included in later research. This is an ongoing project that will see **betterment** over time, to the point where it can be used in localization experiments and other sorts of experiments using the vestibular chair lab of the Biophysics Department of the Radboud University in Nijmegen.

Aknowledgements

A word of thanks to Annemiek Barsingerhorn, Lennaert van der Molen, Jesse Heckman and Kim Wolffenbuttel for technical support in getting to know Matlab, writing the script, conducting the experiments and overall support with doing this internship.

References

- Cesqui, B., Van de Langenberg, R., Lacquaniti, F., & d'Avella, A. (2013). A novel method for measuring gaze orientation in space in unrestrained head conditions. *Journal of vision*, 13(8):28, 1-22.
- Collewijn, H., Erkelens, C., & Steinman, R. (1988). Binocular co-ordination of human horizontal saccadic eye movements. *Journal of Physiology*, 404:157-182.
- Donders, F., & Moore, W. (1864). *On the anomalies of accommodation and refraction of the eye*. London.
- Ferman, L., Collewijn, H., & Van der Berg, A. (1987). A direct test of Listing's law I & II. *Vision Research*, 27(6):929-951.
- Goossens, H., & Van Opstal, A. (1997). Human eye-head coordination in two dimensions under different sensorimotor conditions. *Experimental Brain Research*, 114:542-650.
- Goossens, H., & Van Opstal, A. (2006). Dynamic ensemble coding of saccades in the monkey superior colliculus. *Journal of Neurophysiology*, 95(4):2326-2341.
- Hansen, D., & Ji, G. (2010). In the eye of the beholder: A survey of medels for eyes and gaze. *Transaction on Pattern and Machine Intelligence*, 32(3):478-500.
- Haslwanter, T. (1995). Mathematics of three-dimensional eye rotations. *Vision Research*, 35(12):1727-1739.
- Haslwanter, T., Straumann, K., Hepp, K., Hess, J., & Henn, V. (1991). Smooth pursuit eye movements obey Listing's law in the monkey. *Experimental Brain Research*, 87(2):470-472.

- Hatamian, M., & Anderson, D. (1983). Design considerations for a real-time ocular counterroll instrument. *Transactions on Biomedical Engineering*, 30(5):278-288.
- Helmholtz, H. (1867). *Handbuch der physiologischen optik: Die lehre von den gesichtswahrnehmungen*. Hamburg: Vol 3 Voss Verlag.
- Huynh, D. (2009). Metrics for 3D rotations: Comparison and analysis. *Journal of Mathematical Imaging and Vision*, 35(2):155-164.
- Listing, J. (1845). *Beitrage zur physiologischen Optik*. Göttingen.
- NaturalPoint Inc. (2019). www.optitrack.com/hardware/v120-trio/. Retrieved from www.optitrack.com.
- Otero-Millan, J., Roberts, D., Lasker, A., Zee, D., & Kheradmand, A. (2015). Knowing what the brain is seeing in three dimensions: A novel, noninvasive, sensitive, accurate and low-noise technique for measuring ocular torsion. *Journal of Vision*, 15(14):1-15.
- Pupil Labs GmbH. (2019). www.pupil-labs.com/products/core. Retrieved from www.pupil-labs.com.
- Purves, D., Augustine, G., Fitzpatrick, D., Hall, W., LaMantia, A., McNamara, J., & White, L. (2008). Neuroscience (4th ed.). In D. Purves, *Neuroscience* (pp. 229-282 & 454-467). Sunderland, MA: Sinauer Associates Inc.
- Robinson, D. (1963). A method of measuring eye movement using a scleral search coil in a magnetic field. *Transactions on Biomedical Electronics*, 10(4):137-145.
- Robinson, D. (1964). The mechanics of human saccadic eye movements. *Journal of Physiology*, 174:245-264.
- Ronsse, R., White, O., & Lefèvre, P. (2007). Computation of gaze orientation under unrestrained head movements. *Journal of Neuroscience Methods*, 159(2007):158-169.
- Schiller, P., True, S., & Conway, J. (1980). Deficits in eye movements following frontal eye-field and superior colliculus ablations. *Journal of Neurophysiology*, 44(6):1175-1189.
- Sparks, D. (2002). The brainstem control of saccadic eye movements. *Nature Reviews Neuroscience*, 3:952-964.
- Sparks, D., & Jay, M. (1986). The functional organization of the primate superior colliculus: A motor perspective. *Progress in Brain Research*, 64:235-241.
- Tweed, D., Cadera, W., & Vilis, T. (1990). Computing three dimensional eye position quaternions and eye velocity from search coil signals. *Vision Research*, 30(1):97-110.
- Van Opstal, A., Hepp, K., Suzuki, Y., & Henn, V. (1995). Influence of eye position on activity in monkey superior colliculus. *Journal of Neurophysiology*, 74(4):1593-1610.
- Van Opstal, A., & Van Gisbergen, J. (1989). Scatter in the metrics of saccades and properties of the collicular motor map. *Vision Research*, 29(9):1183-1196.
- Viéville, T., & Masse, D. (2009). Ocular counter-rolling during active head tilting in humans. *Acta Oto-Laryngologica*, 103(3-4):280-290.
- Wade, N., & Tatler, B. (2005). *The moving tablet of the eye: The origins of modern eye movement research*. Oxford: Oxford University Press.

Appendix

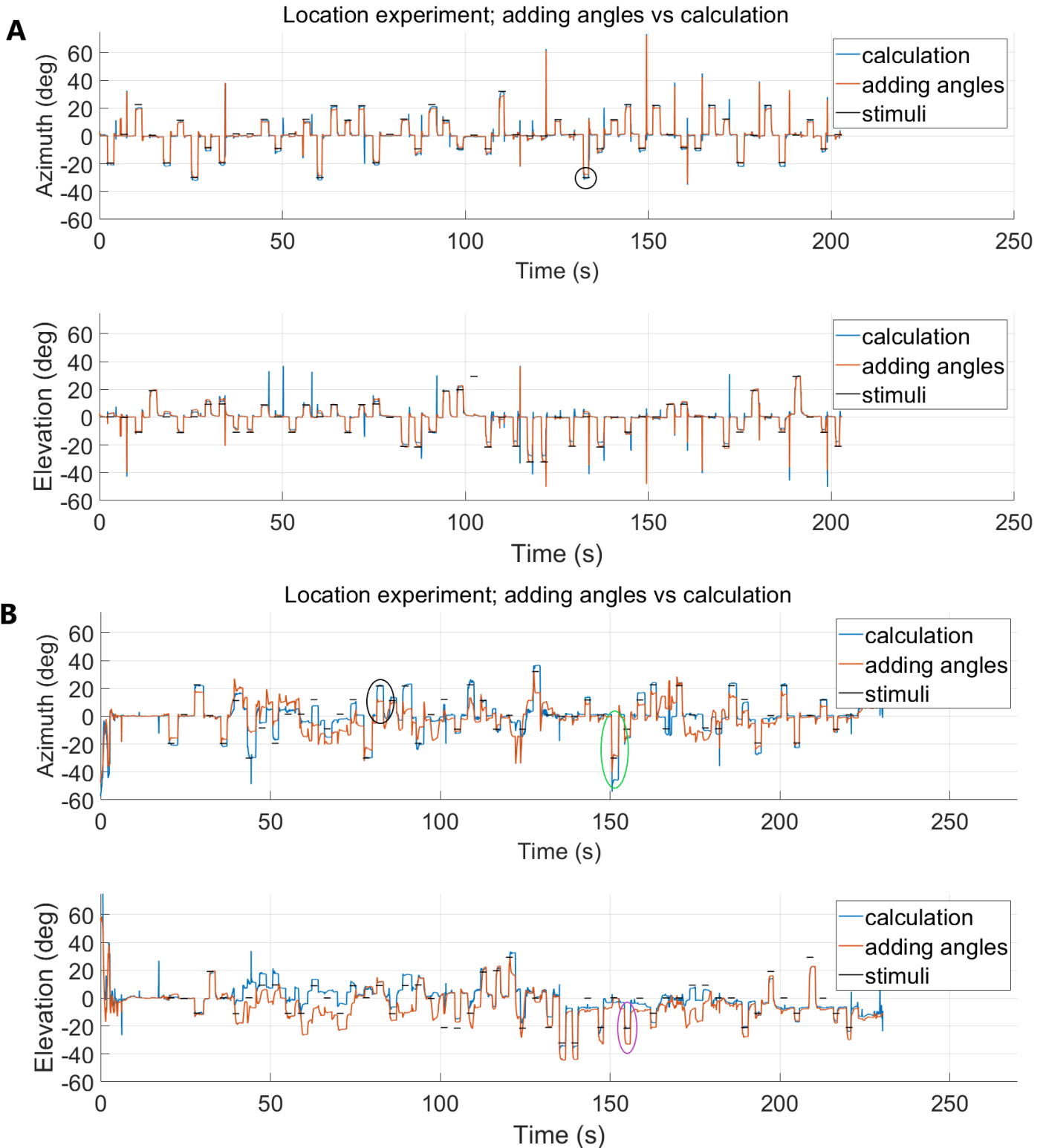


Figure 13 – This figure shows the gaze versus time calculated with quaternions and rotation matrices (blue) and calculated with adding angles of orientation of head and eye. The gaze is measured during a localization experiment where the subject is tasked to make extreme and erratic head movements. The stimuli locations are plotted as small black horizontal lines. For perfect localization, the gaze should be on this line. **A** shows the results from subject KW. In the azimuth graph, the black circle denotes saccade 35, plotted in figure 7A. **B** shows the results of subject MP. Here in the azimuth graph, the black circle denotes saccade 17 and the green circle denotes saccade 35. In the elevation graph, the purple circle denotes saccade 36. These saccades are plotted in figure 7B through 7D respectively.

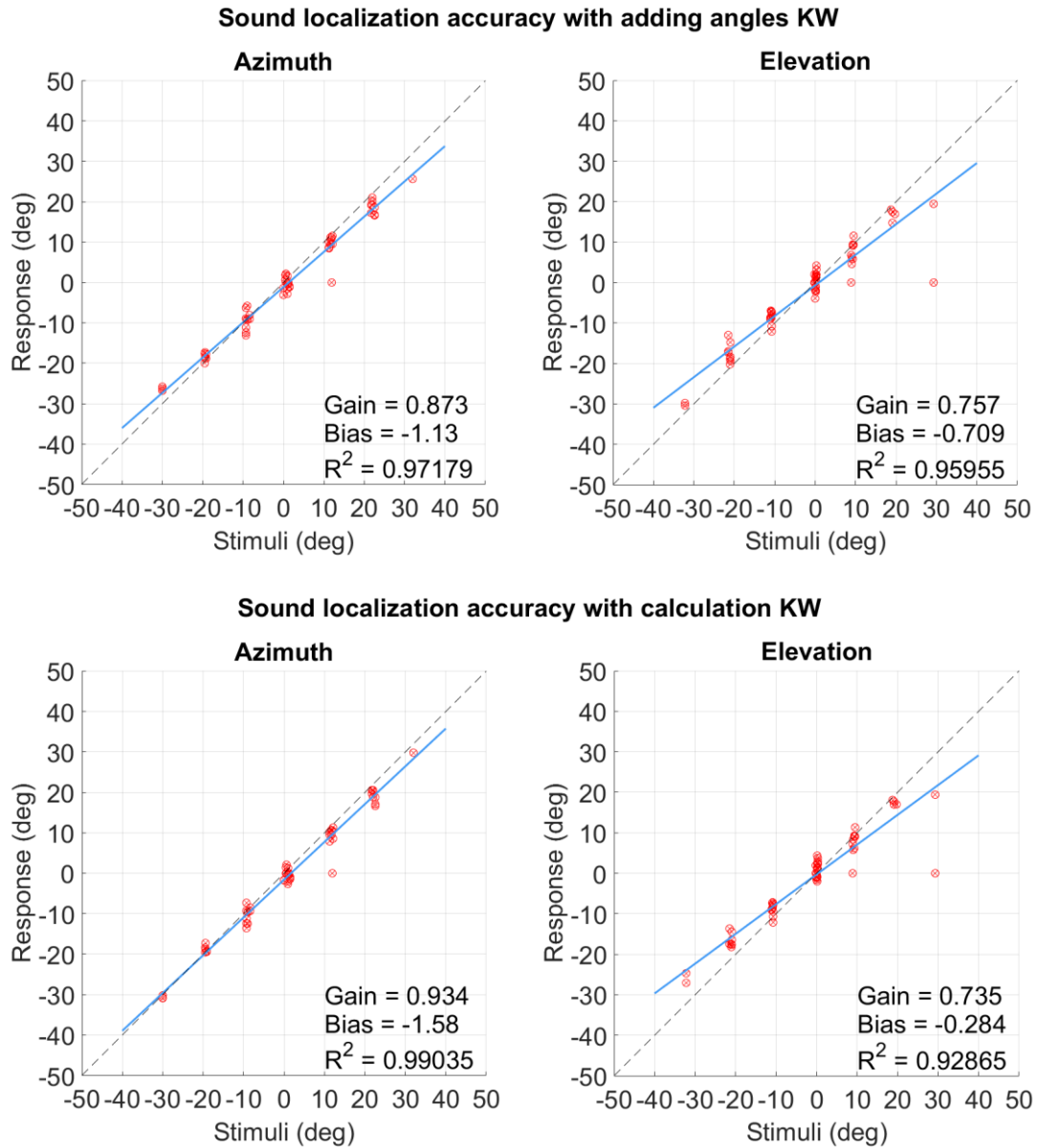
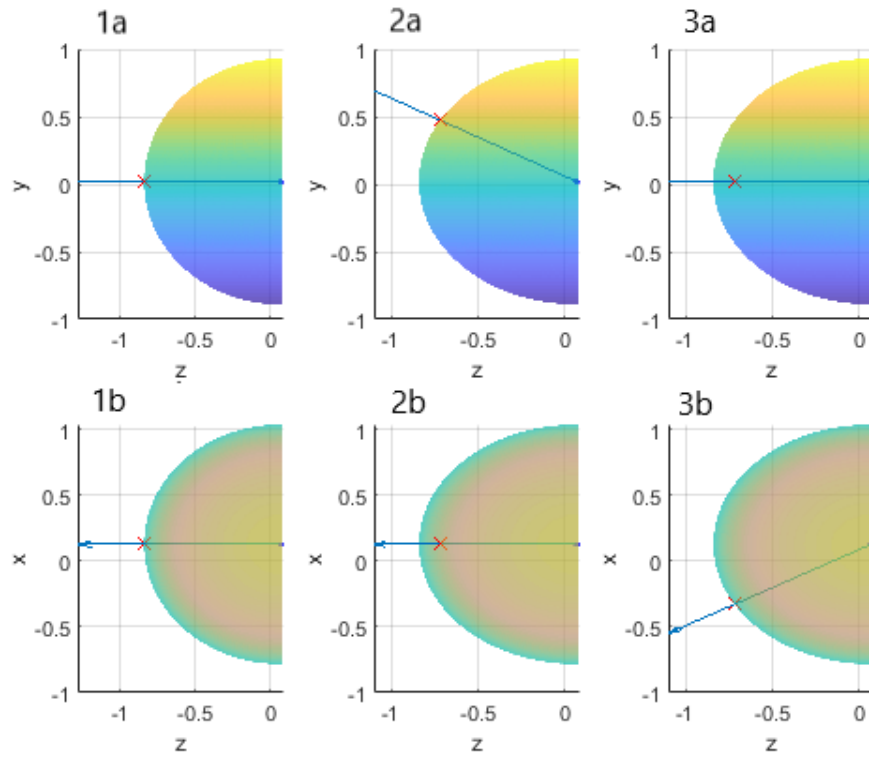


Figure 14 – This figure shows the accuracy of localization of subject KW during the localization experiment where the subject made extreme translational and torsional movements with their head. The response location is plotted against the stimuli location in degrees, both for azimuth (top) and elevation (bottom). The regression line is visible in blue with a dotted black line as the expected regression line. Values for gain, bias and R-squared are added to compare the figures quantitatively.



*Figure 7 – This figure shows the visualization of the calculation of gaze using Fick angles (Ronsse, 2007) given orientation of head and eye and location of head. **1a** and **1b** give a straight gaze for a view from the side (**a**) and a view from above (**b**). For **2a** and **2b** the gaze is 20 degrees up (elevation) for a view from the side (**a**) and a view from above (**b**). For **3a** and **3b** the gaze is 20 degrees to the left (azimuth) for a view from the side (**a**) and a view from above (**b**).*

Scripts

Fick angles

```
function Gaze = Ronsseintersect(locz,locx,locy,Azeye,Eleye,Azhead,Elhead,Torhead)
```

```
%Fill in location of eye in cartesian coordinates (first three parameters)
```

```
%Fill in azimuth and elevation of eye and head respectively (next four
```

```
%parameters
```

```
%Fill in torsion of head (final parameter)
```

```
%Ref frame: z-negative line of sight for straight gaze; x-positive
```

```
%rightwards relative to line of sight for straight gaze; y-positive upwards
```

```
%relative to line of sight for straight gaze (see methods)
```

```
%Radius and location of sphere (fixation LED in sphere)
```

```
R = 0.91;
```

```
locLED = [0.1257,0.0195,-0.8426];
```

```
%Initial coordinates of "eye" relative to location of fixation led
```

```
iniz = locLED(3)+R;
```

```
inix = locLED(1);
```

```
iniy = locLED(2);
```

```
%Parameters of the sphere
```

```
a = 1; b = 1;c = 1;
```

```
calz = 0;
```

```
calx = 0;
```

```
caly = 0;
```

```
%Manual input plus initial location "eye"
```

```
loczax = locz + iniz;
```

```
locxax = locx + inix;
```

```
locyax = locy + iniy;
```

```
%Define angles for calculation of rot matrix (inversions needed to correct
%for rotated reference frame)
```

```
thetah = deg2rad(-Azhead);
```

```
phih = deg2rad(-Elhead);
```

```
psih = deg2rad(Torhead);
```

```
azeye = deg2rad(-Azeye);
```

```
eleye = deg2rad(-Eleye);
```

```
%Length of gaze vector that intersects sphere
```

```
rp = 1.5;
```

```
%Defining eye vector (rotation matrix eye times straight gaze)
```

```
P = [cos(azeye)*cos(eleye), -sin(azeye), cos(azeye)*sin(eleye);...
```

```
sin(azeye)*cos(eleye), cos(azeye), sin(azeye)*sin(eleye);...
```

```
-sin(eleye),0,cos(eleye)] * [rp;0;0];
```

```
Pcal = P + [calz; calx; caly];
```

```
%Defining gaze vector (rotation matrix head times eye vector)
```

```
PG = [cos(thetah)*cos(phih), cos(thetah)*sin(phih)*sin(psih)-sin(thetah)*cos(psih),
cos(thetah)*sin(phih)*cos(psih)+sin(thetah)*sin(psih);...
```

```
sin(thetah)*cos(phih), sin(thetah)*sin(phih)*sin(psih)+cos(thetah)*cos(psih),
sin(thetah)*sin(phih)*cos(psih)-cos(thetah)*sin(psih);...
```

```
-sin(phih), cos(phih)*sin(psih), cos(phih)*cos(psih)] * Pcal;
```

```
%Plotting sphere and gaze vector
```

```
[x, y, z] = sphere(720);
```

```
x = x(360:end,:);
```

```
y = y(360:end,:);
```

```
z = z(360:end,:);
```



```

h = surf((-R*z+(locLED(3)+R))/a^2,(R*x+locLED(1))/b^2,(R*y+locLED(2))/c^2);
set(h,'FaceAlpha',0.5);
shading flat
xlabel('z');ylabel('x');zlabel('y');
hold on

```

```

quiver3(loczax,locxax,locyax,-PG(1),PG(2),PG(3));
[uu, vv, ww] = sphere(64);
kk = surf(0.02*uu+locLED(3)+R,0.02*vv+locLED(1),0.02*ww+locLED(2));
set(kk,'FaceColor',[0 0 1], ...

```

```

    'FaceAlpha',0.1,'FaceLighting','gouraud','EdgeColor','none')

```

```

[u, v, w] = sphere(64);
k = surf(0.02*u+loczax,0.02*v+locxax,0.02*w+locyax);
set(k,'FaceColor',[0 0 1], ...
    'FaceAlpha',0.5,'FaceLighting','gouraud','EdgeColor','none')

```

%Calculating intersection and plotting intersection

```

fun = @(t) (R^2-(((locLED(1))-locxax-PG(1)*t)^2)/a^2 ...
    -(((locLED(2))-locyax-PG(2)*t)^2)/b^2 ...
    -(((locLED(3)+R)-loczax--PG(3)*t)^2)/c^2;
t = roots(chebfun(fun,[0 1]));

```

```

zinter = loczax - PG(1)*t;
xinter = locxax + PG(2)*t;
yinter = locyax + PG(3)*t;

```

```

scatter3(zinter,xinter,yinter,'rx')    %Plotting intersection as red cross

```

%Caluclating gaze in azimuth and elevation in hemisphere reference frame

```

ElGaze = rad2deg(atan2((yinter-locLED(2)),sqrt((xinter-locLED(1))^2+(zinter-(locLED(3)+R))^2)));

```

```
AzGaze = rad2deg(atan2((xinter-locLED(1)),(zinter-(locLED(3)+R))));
```

```
if AzGaze>0
```

```
    AzGaze = AzGaze-180;
```

```
else AzGaze = AzGaze+180;
```

```
end
```

```
Gaze = [AzGaze,ElGaze]
```

```
end
```

Quaternions

```
%% Create AzEl and quaternions for head from Optitrack (Opt) data
```

```
q = quaternion(Opt.qw, -Opt.qx, Opt.qy, -Opt.qz); %Data is given in
```

```
%components of a quaternion (Opt.qx Opt.qy Opt.qz as vectorial part, Opt.qw
```

```
%as scalar part) x and z component are inversed.
```

```
[AzEl]=quat2azelAnnemiek(q); %This function calculates the orientation
```

```
%directly from the quaternion in azimuth and elevation, to use for
```

```
%determining straight gaze later in script
```

```
%% Create AzEl for eye
```

```
%Construction of normal vector
```

```
normv = Pup.gaze_normal_3d(1:10,:);
```

```
normv=median(normv);
```

```
% Estimate rotation matrix
```

```
GG = @(A,B) [ dot(A,B) -norm(cross(A,B)) 0;
```

```
norm(cross(A,B)) dot(A,B) 0;
```

```
0 0 1];
```

```
FFi = @(A,B) [ A (B-dot(A,B)*A)/norm(B-dot(A,B)*A) cross(B,A) ];
```

```
UU = @(Fi,G) Fi*G*inv(Fi);
```

```
b=normv'; a=[0 0 1]';
```

```
Rot = UU(FFi(a,b), GG(a,b));
```

```
% Determine normalized gaze vector
```

```
gaze_normalsrot=Pup.gaze_normal_3d*Rot;
```

```
% Convert to angles azimuth and elevation for determining straight gaze
```

```
% later in the script
```

```
[AzElEye]=-VCxyz2azel(gaze_normalsrot(:,1),gaze_normalsrot(:,2),gaze_normalsrot(:,3));
```

```
%% Create quaternions for Eye
```

```
%First interpolate the normal gaze vector of the eye to be the same length
```

```
%as the Optitrack data
```

```
gaze_normalsrotOpt(:,1)=interp1(lsl_tsPup,gaze_normalsrot(:,1),lsl_tsOpt,'pchip');
```

```
gaze_normalsrotOpt(:,2)=interp1(lsl_tsPup,gaze_normalsrot(:,2),lsl_tsOpt,'pchip');
```

```
gaze_normalsrotOpt(:,3)=interp1(lsl_tsPup,gaze_normalsrot(:,3),lsl_tsOpt,'pchip');
```

```
%Inverse the x and y coordinate to align the Pupillabs data ref frame and the
```

```
%Optitrack data ref frame
```

```
gaze_normalsrotOpt(:,1)=-gaze_normalsrotOpt(:,1);
```

```
gaze_normalsrotOpt(:,2)=-gaze_normalsrotOpt(:,2);
```

```
%Create quaternion for a rotation of straight gaze ([0 0 1]) to the normal
```

```
%gaze vector
```

```
qEye = quaternion.rotateeutov([0 0 1]',gaze_normalsrotOpt',1,1);
```

```
%% Define stimuli
```

```
for j=1:length(BlockInfo.trial)
```

```

        StimAz(j)=BlockInfo.trial(j).stim(2).azimuth;
        StimEl(j)=BlockInfo.trial(j).stim(2).elevation;
end

%% Determine stable fixation towards central LED
% Plotting Raw angles for head and eye
subplot(2,1,1)
plot(Isl_tsOpt,AzEl-AzEl(1,1))
hold on
plot(Isl_tsPup,AzElEye-AzElEye(1,1))
legend('Head azimuth','Head Elevation','Eye azimuth','Eye elevation')
subplot(2,1,2)
plot(Isl_tsOpt,AzEl-AzEl(1,2))
hold on
plot(Isl_tsPup,AzElEye-AzElEye(1,2))
legend('Head azimuth','Head Elevation','Eye azimuth','Eye elevation')

% Determining straight gaze by manually choosing point of straight gaze in
% raw data
[x y]=ginput(1);

[~, indpup]=min(abs(Isl_tsPup-x));
[~, indopty]=min(abs(Isl_tsOpt-x));

%Subtracting median of chosen point of straight gaze to set straight gaze
%to (0,0) azimuth and elevation
AzEye=AzElEye(:,1)-median(AzElEye(indpup-20:indpup+20,1));
ElEye=AzElEye(:,2)-median(AzElEye(indpup-20:indpup+20,2));

AzHead=AzEl(:,1)-median(AzEl(indopt-20:indopt+20,1));
ElHead=AzEl(:,2)-median(AzEl(indopt-20:indopt+20,2));

```

```

%Creating rotation matrices for multiplied quaternion data with their
%respective straight gaze quaternions

qRot = q(indopt);
qRotEye = qEye(indopt);
RsEye = RotationMatrix(qEye*qRotEye');
Rs = RotationMatrix(q*qRot');

%% Interpolate eyedata to Optitrack length and remove values with low confidence for eye data
AzEyeinterp=interp1(lsl_tsPup(Pup.confidence>0.7),AzEye(Pup.confidence>0.7),lsl_tsOpt,'pchip');
ElEyeinterp=interp1(lsl_tsPup(Pup.confidence>0.7),ElEye(Pup.confidence>0.7),lsl_tsOpt,'pchip');

%Transpose to get correct size
AzEyeinterp = AzEyeinterp';
ElEyeinterp = ElEyeinterp';

%% Calculate gaze in azimuth and elevation
% Calibration data (only radius is being used)
R=0.85;

% Calculating Gaze vectors with matrix multiplication
tic
for n = 1:length(lsl_tsOpt)
    P(:,n) = RsEye(:,1,n) * [0;0;1]; %multiplying the eye rot matrix with a straight gaze of
    % [0,0,1] to create eye vector (eye in head)
    Pcal(:,n) = P(:,n)
    PG(:,n) = Rs(:,1,n) * Pcal(:,n); %multiplying rot matrix of head data with eye vector to
    %create gaze vector (eye in world)
    PGs(:,n) = PG(:,n)*2+[-(Opt.x(n)-Opt.x(indopt)); (Opt.y(n)-Opt.y(indopt)); -(Opt.z(n)-
    Opt.z(indopt))]; %adjusting for translations of the eye all location data is relative to the
    %initial straight gaze position (Opt.X(indopt)) and x and z data is inversed to adjust for %the
    correct ref frame
    PGnorms(:,n)=PGs(:,n)/norm(PGs(:,n)); %normalizing gaze vectors

```

```
%Intersecting the normalized gaze vector with the hemisphere
```

```
vector(:,n)=[linspace(-(Opt.x(n)-Opt.x(indopt)),PGs(1,n),1000);linspace((Opt.y(n)-  
Opt.y(indopt)),PGs(2,n),1000);linspace(-(Opt.z(n)-Opt.z(indopt)),PGs(3,n),1000)];
```

```
[~,intersect(n)]=min(abs((vector(1,:,n).^2+vector(2,:,n).^2+vector(3,:,n).^2)-R^2));
```

```
PGintersect(:,n)=vector(:,intersect(n),n);
```

```
end
```

```
toc
```

```
% Calculating gaze in azimuth and elevation from gaze vector
```

```
[AzElGaze]=-VCxyz2azel(PGintersect(1,:),PGintersect(2,:),PGintersect(3,:));
```

```
AzGaze=AzElGaze(:,1);
```

```
ElGaze=AzElGaze(:,2);
```

```
% Exlcuding outliers
```

```
AzGaze(AzGaze>80 | AzGaze<-80)=NaN;
```

```
ElGaze(ElGaze>80 | ElGaze<-80)=NaN;
```

```
% Calculating reference gaze (old method, simply adding angels) and exclude
```

```
% outliers
```

```
AzGazecheck = AzHead - AzEyeinterp;
```

```
AzGazecheck(AzGazecheck>80 | AzGazecheck<-80)=NaN;
```

```
ElGazecheck = -ElHead - ElEyeinterp;
```

```
ElGazecheck(ElGazecheck>80 | ElGazecheck<-80)=NaN;
```